

STRUCTURAL EVOLUTION OF RUNDVÅGSHETTA REGION, LÜTZOW-HOLM BAY, EAST ANTARCTICA

Masahiro ISHIKAWA¹, Yoichi MOTOYOSHI², Geoffrey L. FRASER³
and Toshisuke KAWASAKI⁴

¹*Institute of Geology and Paleontology, Faculty of Science,
Tohoku University, Sendai 980-77*

²*National Institute of Polar Research, 9-10, Kaga 1-chome,
Itabashi-ku, Tokyo 173*

³*Research School of Earth Sciences, Australian National University,
Canberra, ACT 0200, Australia*

⁴*Department of Earth Science, Faculty of Science,
Ehime University, Matsuyama 790*

Abstract: The highest grade part of the Lützow-Holm Complex crops out on the southern coastline of Lützow-Holm Bay in East Antarctica. Orthopyroxene + sillimanite ± quartz assemblages reveal high-*T*, high-*P* conditions for peak metamorphism of granulites of Rundvågshetta. Moreover, their fabrics imply regional ductile deformation during peak metamorphism, which was characterized by the formation of a WNW-ESE subhorizontal mineral lineation and the development of high-strain structures such as isoclinal buckling folds (F_n) and boudinage (B_n and B_m). The high-strain deformation was followed by the development of symplectic intergrowths of cordierite ± sapphirine ± spinel around sillimanite and orthopyroxene, and symplectic intergrowths of orthopyroxene + cordierite ± sapphirine around garnets in response to decompression. There is little symplectic intergrowth strained intensely, whereas strained cordierite is locally observed. It implies that the regional high-strain deformation had ceased before the time of the reactions orthopyroxene + sillimanite + quartz = cordierite, orthopyroxene + sillimanite = cordierite + sapphirine ± spinel, garnet = orthopyroxene + cordierite + sapphirine and garnet + quartz = orthopyroxene + cordierite.

In contrast to the peak metamorphic high-strain deformation, the post-peak metamorphic structural evolution was characterized by low-strain and localized deformations such as F_{n+1} gentle folding, emplacement of clinopyroxene pegmatites and basic dykes, and local shearing in the N-S compressional and E-W extensional field. In response to subsequent N-S compression, ductile thrusting had taken place. The last structural event at Rundvågshetta was represented by the emplacement of felsic pegmatites.

1. Introduction

The Lützow-Holm Complex, a granulite- to amphibolite-facies metamorphic complex, is exhumed along the Lützow-Holm Bay and the Prince Olav Coast, East Antarctica (HIROI *et al.*, 1991). During the last forty years, many geologists have surveyed these areas, and the Complex have been well characterized geologically and petrologically (YOSHIDA, 1978 ;

HIROI *et al.*, 1983, 1986, 1987; MOTOYOSHI, 1986; SHIRAISHI *et al.*, 1987). As a summary of those previous works, MOTOYOSHI *et al.* (1989) proposed a clockwise *P-T* path and estimated approximately 760°–830°C at 0.7–0.8 GPa for regional granulite-facies metamorphism on the basis of geothermobarometry. KAWASAKI *et al.* (1993) have reported orthopyroxene+sillimanite±quartz assemblages with cordierite as a reaction product during decompression after the peak metamorphism, and MOTOYOSHI *et al.* (1993) have revised the peak conditions to be >900°C at nearly 1.0 GPa. Moreover, SHIRAISHI *et al.* (1994) reported ~500 Ma for regional metamorphism in Lützow-Holm Bay and Prince Olav Coast (521 Ma from Rundvågshetta) by the U-Pb SHRIMP method, and proposed that the Lützow-Holm Complex is not a portion of a Proterozoic terrain but belongs to a Cambrian orogenic belt whereas older ages, 3020 Ma by Rb-Sr whole rock isochron method (NAKAJIMA *et al.*, 1988) and 2500–2800 Ma for zircon core by U-Pb SHRIMP method (SHIRAISHI *et al.*, 1994) have also been reported.

The detailed structural evolution of the region is not yet fully understood, although regional structural geology of the Lützow-Holm Bay have been described (ISHIKAWA, 1976; ISHIKAWA *et al.*, 1976, 1977; YOSHIDA, 1977, 1978; MATSUMOTO *et al.*, 1979, 1982).

In this paper, we newly report (1) intense ductile deformation during orthopyroxene+sillimanite±quartz metamorphic conditions, (2) local preferred orientation of secondary cordierite, which is interpreted to have developed during low-strain deformation, and (3) multiple deformation phases, and discuss the relationship between metamorphic reactions and modes of deformation observed in orthopyroxene-sillimanite bearing lithologies from Rundvågshetta (39°00′–04′E, 69°54′S). We present a detailed structural event history for Rundvågshetta which will provide the essential context in which to interpret future petrological and chronological studies in the region.

2. General Geology

Rundvågshetta is underlain by various kinds of well-layered metamorphic rocks, which are mainly composed of garnet-sillimanite gneisses, garnet-biotite gneisses, pyroxene gneisses with subordinate calc-silicates (unpublished). Pyroxene gneisses are the most common lithology, while intercalated garnet-biotite and garnet-sillimanite gneisses predominate in the northern area. The critical evidence discussed here comes from cordierite-bearing lithologies which occur within garnet-sillimanite and garnet-biotite gneisses in the northern part of Rundvågshetta (Fig. 1). In contrast to voluminous metamorphic rocks, intrusives are less voluminous. Metamorphic rocks commonly exhibit compositional layering parallel to lithological boundaries, which strike generally WNW-ESE and dip to the south at 50°–70° in the southern and central area. In contrast, the regional strikes are disturbed in the northern area due to a mappable gentle antiform and dip angles are rather low (30°–10°). The fold axis of the mappable antiform plunges nearly ESE at 30°–10°, and the axial plane dips subvertically. In the northern part, mesoscopic gentle folds associated with the mappable upright antiform, are well-developed and exhibit axial planar foliations defined by aligned biotite grains in garnet-biotite gneiss and pyroxene gneisses. Most metamorphic rocks exhibit mineral lineations defined by sillimanite, orthopyroxene, hornblende and quartz. The trend of lineations is WNW to ESE plunging at low angles. The trend is parallel to the fold axes of numerous mesoscopic

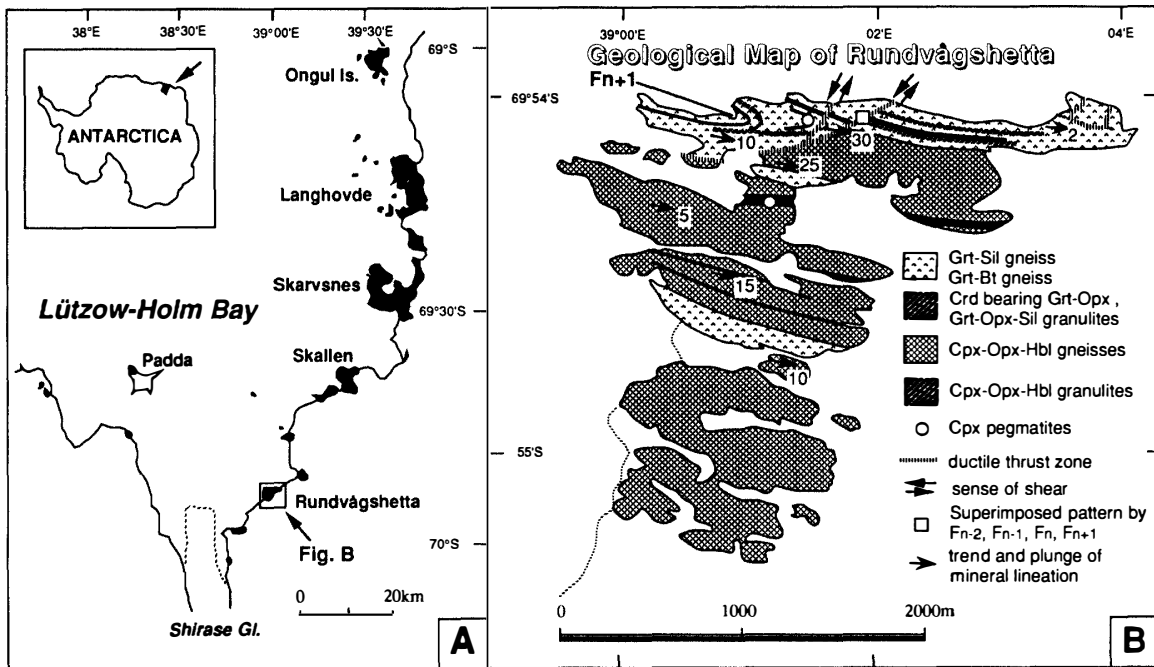


Fig. 1. Location map and geological map of Rundvågshetta. A: Location of Rundvågshetta in Lützow-Holm Bay, East Antarctica. B: Structural map of Rundvågshetta. The geological map is simplified and modified after MOTOYOSHI *et al.* (1986) and KAWASAKI *et al.* (1993).

isoclinal folds. There are several mappable ductile thrusts and associated strike-slip ductile shear zones striking W-E to NE-SW in the northern part (Fig. 1B) where the dominant mineral lineations are locally disturbed.

3. Lithology

Rheological behaviors of metamorphic rocks are highly dependent on modal proportions of the constituent minerals. Therefore in order to discuss the structural evolution, we distinguish the following rock types based on modal proportion of the constituent minerals. In this paper we use “granulite” as a weak- or non-foliated granulite-facies rock while we use “gneiss” as a rock exhibiting gneissose texture. Mineral abbreviations are used after KRETZ (1983).

The most common rock type at Rundvågshetta is a pyroxene gneiss, which is composed mainly of Cpx, Opx, Hbl, Bt, Pl, Kfs and Qtz. On the basis of modal proportion, it is subdivided into two types. The first is a foliated, medium-grained Cpx-Opx-Hbl gneiss with abundant Pl, Kfs and Qtz. This gneiss commonly hosts boudinaged lenses. The other is a weakly-foliated, medium to coarse-grained Cpx-Opx-Hbl granulite with minor Bt, Pl, Kfs and Qtz. This lithology occurs as continuous layers or discontinuous-concordant lenses within Cpx-Opx-Hbl gneiss.

Medium-grained Grt-Sil-Bt-Pl-Kfs-Qtz gneisses occur as thin, continuous and concordant layers within pyroxene gneisses in the central to southern part, and occur as thick, continuous and concordant layers (up to several tens of meters in thickness) in the northern

part of Rundvågshetta. The gneiss locally contains secondary Crd.

Gr_t+Opx+Sil assemblages are common at Rundvågshetta, and secondary Crd and a variety of symplectites are found in this rock type (KAWASAKI *et al.*, 1993; MOTOYOSHI *et al.*, 1993). It is subdivided into three types. One type is a Gr_t-Opx-Sil gneiss with major Pl, Kfs, Qtz and secondary Crd. The abundance of Qtz is characteristic of this gneiss. The Gr_t-Opx-Sil gneiss is found locally as thin layers in the northern part of Rundvågshetta. A second type is a coarse-grained Gr_t-Opx granulite with minor Sil, Pl and Qtz, and secondary Spr, Spl, Crd, Opx and Bt. The granulite occurs as thin layers or boudinaged lenses within Gr_t-Sil gneisses in the northern part of Rundvågshetta. A third type is a coarse to medium-grained Gr_t-Opx-Sil granulite with minor Pl, Kfs, Qtz and secondary Spr, Spl, Crd, Opx, Bt. The Gr_t-Opx-Sil granulite occurs locally as thin layers within Gr_t-Sil gneisses in the northern part of Rundvågshetta.

4. Fabrics and Reaction Textures

Metamorphic rocks from Rundvågshetta exhibit linear and planar fabrics, and many reaction textures are observed. Planar fabrics are subdivided into compositional layering and foliation defined by aligned Bt grains. The dominant mineral lineation is postdated by metamorphic reaction textures involving the breakdown of primary minerals.

4.1. Planer fabric

4.1.1. Compositional layering

Most metamorphic rocks show compositionally banded foliations due to variation in modal proportion of primary minerals, which are generally parallel to lithological boundaries. The compositional foliation is characterized by the alternation of Gr_t-Sil-Bt-rich and Pl-Kfs-Qtz-rich parallel layers in Gr_t-Sil gneiss, Opx-Sil-rich and Qtz-Pl-Kfs-rich parallel layers in Opx-Sil gneiss, and Cpx-Opx-Hbl-Bt-rich and Pl-Kfs-Qtz-rich layers in Cpx-Opx-Hbl gneiss. Distinct Gr_t-rich and Sil-rich layers are found in some Gr_t-Sil gneisses (Fig. 2). Each layer ranges from several millimeters to several cm in thickness. This compositional banded foliation is parallel to mineral lineation.

4.1.2. Aligned biotite grains

In the Gr_t-Bt gneiss and Cpx-Opx-Hbl-Bt gneiss, Bt defines a later foliation which is subvertical and oblique to compositional layering. This Bt fabric is axial planar to upright F_{n+1} folds (see Section 5)

4.2. Mineral lineation

The metamorphic rocks have a granoblastic to elongate-fabric, which is generally symmetrical and parallel to compositional layering, axes of F_n isoclinal folds and elongation axes of B_n ductile boudinage (see Section 5). The elongate-texture in the Cpx-Opx-Hbl gneiss and Cpx-Opx-Hbl granulite is characterized by weakly-elongate mineral grains (*e.g.*, pyroxenes and Hbl). Gr_t-Sil gneiss commonly shows a strong mineral lineation, defined by Qtz, Sil (Fig. 3) and Gr_t. As well as most lithologies, Opx-Sil gneiss also shows strong elongate-fabrics characterized by preferred orientation of Sil, Qtz and Opx. Because Opx+Sil+Qtz assemblage from Rundvågshetta represents a high-*P* high-*T* (peak metamorphic) conditions (KAWASAKI *et al.*, 1993), the formation of these dominant

Fig. 2. Intense foliation defined by alternation of Grt-rich and Sil-rich bands in Grt-Sil gneiss.

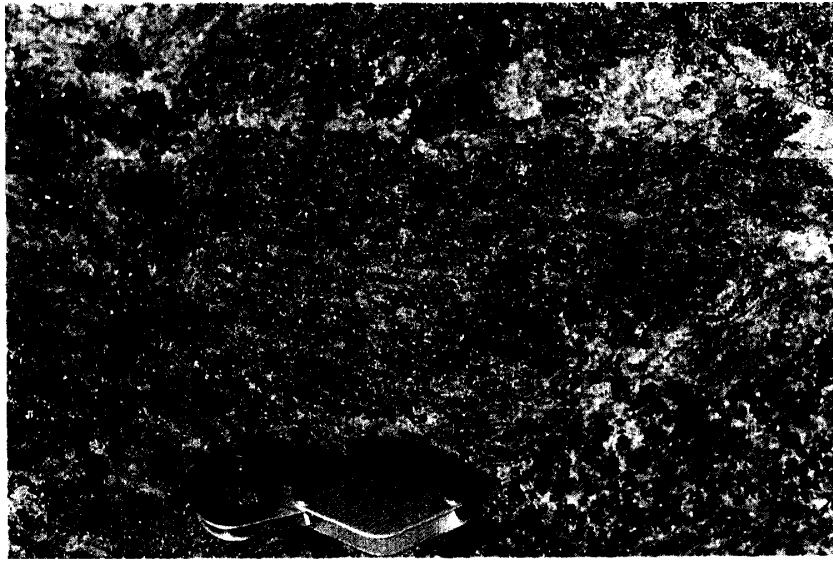


Fig. 3. Photomicrograph of strong preferred orientation, which is defined by Sil in Grt-Sil gneiss. Plane polarized light. Sample no. J34-RN84-4.

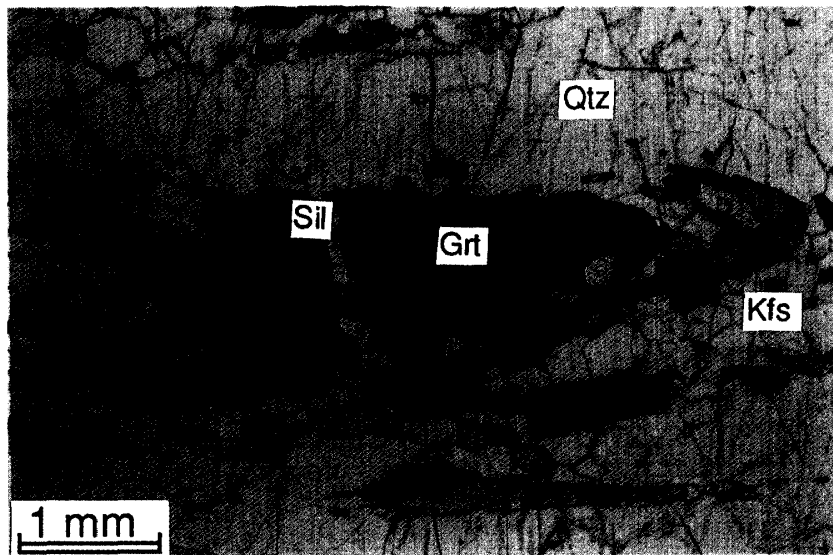
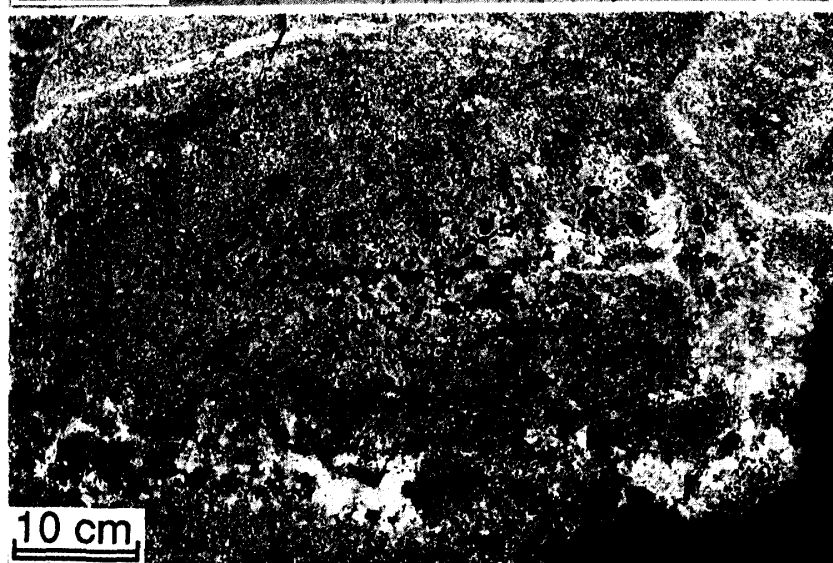


Fig. 4. Mineral reaction texture in Grt-Opx granulite. A variety of reaction textures have been produced around Grt.



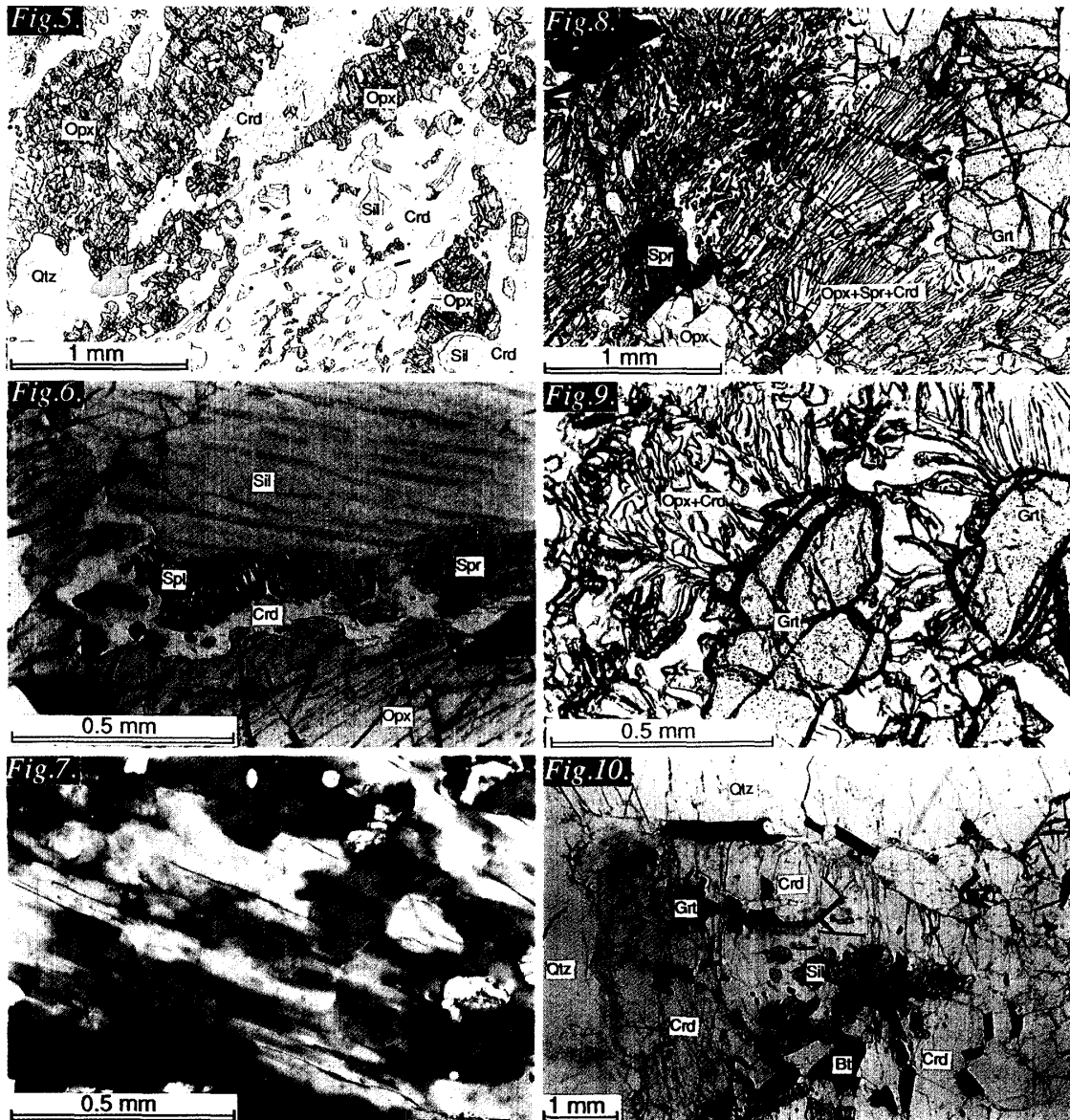


Fig. 5. Photomicrograph of secondary Crd in Opx-Sil gneiss. Opx, Sil and Qtz, never in direct contact, are observed to have broken down to Crd, according to the reaction: $Opx + Sil + Qtz = Crd$. Plane polarized light. Sample no. J34-RN85-5.

Fig. 6. Photomicrograph of Crd + Spr + Spl symplectite, which separates Opx from Sil in Qtz-absent domain of Grt-Opx granulite. Inferred possible reaction is $Opx + Sil = Crd + Spr + Spl$. Plane polarized light. Sample no. RVH93010601-X.

Fig. 7. Photomicrograph of preferred orientation of secondary Crd. Cross polarized light. Sample no. J34-RN85-5.

Fig. 8. Photomicrograph of Opx + Crd + Spr symplectite after Grt in Grt-Opx granulite. Inferred possible reaction is $Grt = Opx + Crd + Spr$. Plane polarized light. Sample no. RVH93010601-X.

Fig. 9. Photomicrograph of Opx + Crd symplectite around Grt in Qtz-present domain of Grt-Opx granulite. Inferred possible reaction is $Grt + Qtz = Opx + Crd$. Plane polarized light. Sample no. RVH93010601-X.

Fig. 10. Photomicrograph of secondary Crd in Grt-Sil gneiss. Crd mantles Grt, Sil and Qtz which are never in direct contact. On the basis of the textures, the reaction, $Grt + Sil + Qtz = Crd$, is inferred. Plane polarized light. Sample no. J34-RN96-052001.

mineral lineations probably occurred during peak metamorphism. Here we defined the dominant mineral lineation as L_n lineation.

4.3. Reaction texture

In the Grt-Sil gneiss, Grt-Opx-Sil gneiss, Grt-Opx-Sil granulite and Grt-Opx granulite, many reaction textures are formed by the break down of primary minerals (Fig. 4).

Opx and Sil are never in direct contact with each other and appear to have reacted to form Crd, $\text{Crd} + \text{Spr}$, according to the reactions:



R1 explains Crd+Spr symplectites in Qtz-absent domains, and R2 explains Crd in Qtz-present domains of Grt-Opx-Sil gneiss (Fig. 5), Grt-Opx granulite and Grt-Opx-Sil granulites (KAWASAKI *et al.*, 1993; MOTOYOSHI *et al.*, 1993). Moreover following reaction :



may explain Crd+Spr+Spl symplectites, which separate Opx from Sil in Qtz-absent domains of Grt-Opx granulite (Fig. 6). The secondary Crd shows preferred orientation in places (Fig. 7) which is subparallel to the Sil lineation, and occasionally at low to moderate angle to compositional bands.

In Grt-Opx granulite and Grt-Opx-Sil granulite, Grt is mantled by $\text{Opx} + \text{Crd} \pm \text{Spr}$ symplectites (Figs. 8 and 9). The following reactions are inferred ;



and



These reactions are described by KAWASAKI *et al.* (1993). The $\text{Opx} + \text{Crd} + \text{Spr}$ and $\text{Opx} + \text{Crd}$ symplectites are generally undeformed in the Grt and Opx-rich domains, but we locally found deformed reaction textures in the Crd-rich domain.

In some Grt-Sil gneisses, Crd mantles Grt, Sil and Qtz, which are never in direct contact (Fig. 10). From the textures, the following reaction is probably inferred ;



The Crd domain exhibits granoblastic texture, and does not show preferred orientation.

As discussed elsewhere (KAWASAKI *et al.*, 1993, MOTOYOSHI *et al.*, 1993), all these metamorphic reactions suggest nearly isothermal decompression after the peak metamorphic conditions.

5. Structural Evolution

Structural evolution of Rundvågshetta is subdivided into an early intense ductile deformation and a late weak and localized deformation. The early intense ductile deformation was characterized by the development of isoclinal folds and ductile boudinage. The late structural evolution was represented by the development of open to

gentle folds, the intrusion of Cpx pegmatites and basic dykes associated with local extensional cracking, the formation of extensional-narrow-ductile shear zone and associated extensional-conjugate-brittle fault, ductile thrusting and intrusion of pegmatite.

5.1. Intense ductile deformation

Metamorphic rocks of Rundvågshetta have been affected by early intense deformation represented by dominant isoclinal folds and ductile boudinage. The detailed descriptions of early intense deformations are as follows.

5.1.1. F_n folding and pre- F_n folding

Lithological boundaries and the compositional layering have been intensely folded throughout Rundvågshetta. The fold axes are parallel to the dominant L_n mineral lineation, suggesting that the intense folding occurred contemporaneously with formation of the L_n lineation. Therefore we defined this folding phase as F_n . The F_n folding is a dominant folding phase, and forms tight to isoclinal folds with subhorizontal fold axes and steep axial surfaces, except in the northern part where recumbent isoclinal folds with subhorizontal axial surfaces are observed due to late folding (Fig. 11). The amplitude of F_n folds range from several millimeters to several tens of meters. The wavelength of F_n folds ranges from several millimeters to several tens of meters, depending on lithological layer thickness, indicating F_n folds are buckled-folds (Fig. 12). The asymmetry of mesoscopic (1–10 m) folds indicates that the first order enveloping surfaces of F_n folds dip southward in the Rundvågshetta area. Aligned Bt grains in Grt-Bt gneiss, Cpx-Opx-Hbl gneisses and Cpx-Opx-Hbl granulites crosscut the fold axial surfaces of F_n folds, suggesting that the aligned Bt grains have been produced after the time of formation of F_n folds. Axial surfaces of F_n folds were disturbed by subsequent F_{n+1} folding.

Due to the intense fabrics recrystallised at high metamorphic grade during F_n folding, preexisting deformation fabrics are difficult to recognize. However, we recognize evidence for two ductile deformation phases which predate F_n folding at one outcrop in the northern part of Rundvågshetta. At this outcrop, a vertical rock wall approximately 4 meters high preserves complex fold interference patterns as shown in Figs. 13 and 14. The development of such interference patterns requires at least two isoclinal folding phases, F_{n-1} and F_{n-2} which are overprinted by F_n and finally by F_{n+1} folds. Intense recrystallization during the F_n folding phase has obscured the relationship between F_{n-1} , F_{n-2} and metamorphism.

5.1.2. Ductile boudinage

Relatively competent lithologies (e.g. Cpx-Opx-Hbl granulite intercalated with Cpx-Opx-Hbl gneiss, Grt-Opx granulite intercalated with Grt-Sil gneiss) occur as symmetrically boudinaged lenses, indicating strong ductile boudinage (Fig. 15). Generally they exhibit normal boudins (see HOBBS *et al.*, 1976). The elongate-axes of ductile boudinage are parallel to the preferred orientation of the dominant L_n mineral lineation. Elongated Sil developed at the necking part of boudinaged Grt-Opx-Sil granulite. Therefore the formation of the dominant L_n mineral lineation and the ductile boudinage are considered to be coeval. Here the ductile boudinage phase is defined as B_n . In the central and marginal parts of boudinaged lenses of Grt-Opx granulite and in neighboring Pl-rich hosts, a number of undeformed Opx + Crd \pm Spr symplectic textures are recognized, suggesting that B_n ductile boudinage phase ceased before the time of formation of Opx + Crd \pm Spr



Fig. 11. F_n fold. The most dominant folds are tight to isoclinal folds.



Fig. 12. F_n fold, which is typically high-strained buckled-fold. Width of photo = 20 cm.



Fig. 13. Superimposed fold pattern, formed by F_{n-2} , F_{n-1} , F_n and F_{n+1} folds. Height of outcrop = 4 m.

symplectites. In contrast to competent layers, relatively incompetent lithologies were folded in the neighboring part due to the B_n boudinage. The gentle folds associated with boudinage are distinguished from F_{n-2} , F_{n-1} , F_n and F_{n+1} folds, and we do not label them in this paper.

In addition to B_n boudinage, relatively competent lithologies exhibit chocolate block boudins (see HOBBS *et al.*, 1976) in places. They were formed by interference pattern of neck lines of B_n boudinage and B_m symmetrical ductile boudinage of which the elongation-orientation is perpendicular to L_n mineral lineation. The occurrence of both B_n and B_m boudinages indicates that there has been strong stretching both parallel and perpendicular to the L_n mineral lineation in the axial planes of F_n fold. Although there is no convincing evidence of the relative timing of B_n and B_m , we can see timing relationships between boudinage and fold generations. Hinges of F_n fold were locally boudinaged by the B_n boudinage (Fig. 16) and B_m boudinage. This field correlation implies that B_n and B_m ductile boudinage took place during the late stage of F_n folding (subsequent flattening) under the peak metamorphic conditions.

The plunge of neck-lines of B_n and B_m boudinages are weakly disturbed by gentle folds (F_{n+1}) in places. In addition, the upright gentle folds of smaller scale can be seen in the neck region of B_n boudins (Fig. 17). This structure suggests that the B_n and B_m boudins predate the F_{n+1} folding phase.

5.2. Weak and local deformation

Metamorphic rocks of Rundvågshetta have been affected by the late weak and localized deformation which is represented by gentle folds, emplacement of Cpx pegmatite and basic dyke, extensional narrow shear zone formation, ductile thrust formation and emplacement of felsic pegmatite. The detailed descriptions are as follows.

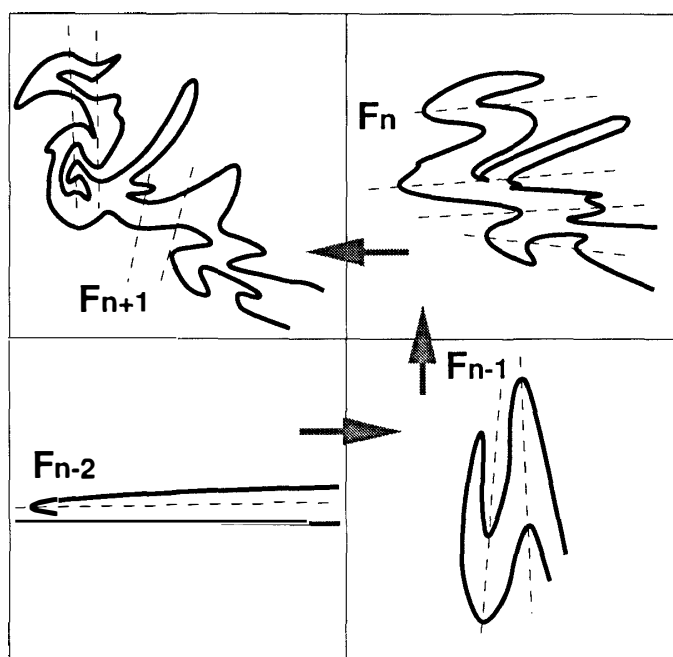


Fig. 14. Development of superimposed fold pattern.

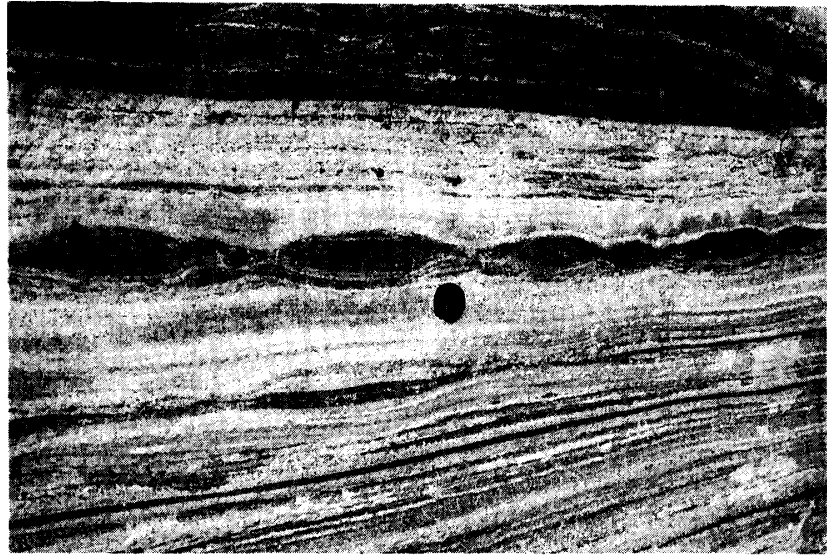


Fig. 15. B_n boudinage. Grt-Opx granulites are typically boudinaged during the B_n phase.



Fig. 16. Boudinaged F_n hinge in Grt-Opx granulite, indicating that the B_n boudinage has been produced after the F_n folding phase or in a single prolonged high-strain deformation phase.



Fig. 17. B_m boudinage, folded by F_{n+1} . This structure suggests that the B_m boudinage has been produced before F_{n+1} folding phase. Width of photo = 2 m.

5.2.1. F_{n+1} folding

The regional strikes of lithological boundaries are slightly re-oriented by the result of a post- F_n deformation episode. The F_{n+1} folds are gentle to open folds with subvertical axial planes striking nearly E-W with subhorizontal fold axes (Fig. 18), suggesting relatively low strain during N-S compression. The fold axes of F_{n+1} are parallel or subparallel to those of the F_n and the dominant mineral lineations. The amplitude of F_{n+1} folds ranges from several tens of cm to several tens of meters and the wavelength ranges from several tens of cm up to several hundreds of meters. The axial planes of F_{n+1} folds are commonly defined by foliations of Bt in Grt-Bt gneisses (Figs. 19 and 20), implying that the preferred orientation of Bt has been produced during the formation of F_{n+1} .

5.2.2. Emplacement of Cpx pegmatite and basic dyke and extensional cracking

Two intrusives, associated with extensional cracking, have been recognized. The first phase is called Cpx pegmatite. The major constituent is Cpx, and a minor amount of Hbl and Pl are contained. The Cpx pegmatites were intruded into N-S trending subvertical ruptures which are perpendicular to the L_n mineral lineation (Figs. 21 and 22), and are restricted to relatively strong pyroxene-abundant granulites (*e.g.* Cpx-Opx-Hbl granulite) or alternation zones of them. The second phase is a set of basic dykes consisting of Cpx, Hbl and Pl (MOTOYOSHI *et al.*, 1986). The basic dykes were intruded into N-S trending subvertical ruptures perpendicular to the L_n mineral lineation (Fig. 23). In contrast to Cpx pegmatite, basic dykes cut all kinds of lithologies. Both phases of intrusives cut F_n and F_{n+1} folds (Fig. 24) but are in places slightly folded with subvertical fold axial planes parallel to axial planes of F_{n+1} folds (Fig. 25). This suggests that these intrusives were emplaced in an E-W extensional and N-S compressional stress field in the latter stages of the F_{n+1} folding phase. Basic dykes are locally sheared by extensional narrow ductile shear zones (Fig. 26). Thus it is apparent that basic dyke intrusion took place before extensional narrow shearing (see below).

5.2.3. Extensional, conjugate, narrow ductile shear zone and fault formation

Deformation subsequent to Cpx pegmatite and basic dyke intrusion is characterized by E-W extensional shear zones (Figs. 27, 28 and 29) which cut subvertically at moderate angles to the pre-existing foliations. In quartzo-feldspathic gneisses (*e.g.* Cpx-Opx-Hbl gneiss, Grt-Bt gneiss, Grt-Sil gneiss) extension produced narrow ductile shear zones, whereas in pyroxene-rich granulites (*e.g.* Cpx-Opx-Hbl granulite) brittle faults were produced. Due to the narrow ductile shearing, the pre-existing foliations and the dominant mineral lineation were dragged and strikes of foliations were gradually re-oriented to be parallel to the new penetrative foliation and lineation in quartzo-feldspathic gneisses (*e.g.* defined by Sil grains in Grt-Sil gneiss). The observation that new lineations of Sil and Qtz are formed along narrow ductile shear zones in Grt-Sil gneiss, suggests that Grt + Sil + Qtz assemblage was still stable during the phase of local development of ductile shear zones. In contrast to narrow ductile shear zones, conjugate faults cut the pre-existing foliation and the dominant mineral lineation of pyroxene-abundant granulites (*e.g.* Cpx-Opx-Hbl granulite), and the layers and B_n -boudinaged lenses of pyroxene-abundant granulites were brittlely boudinaged by the extensional conjugate faults. Conjugate systems of narrow ductile shear zones and brittle faults tend to develop well in the intercalated zones of pyroxene-abundant granulites and quartzo-feldspathic gneisses. The conjugacy indicates an E-W extensional and N-S compressional stress field. The same

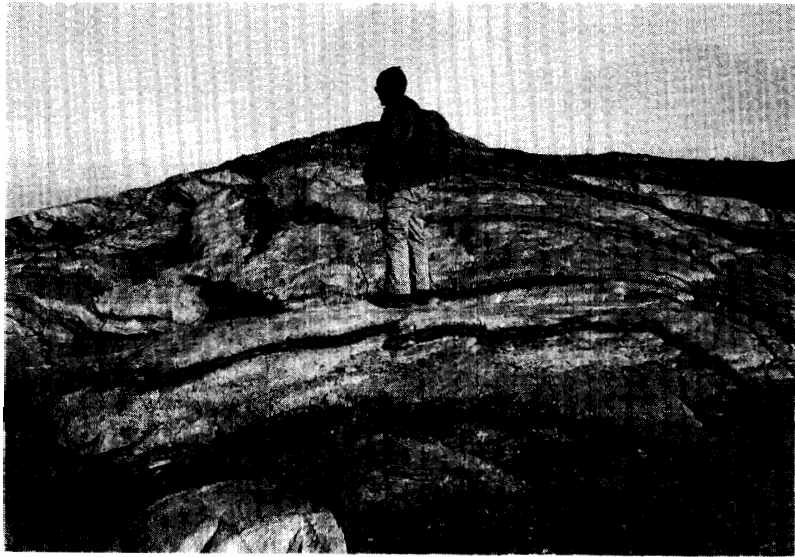


Fig. 18. Gentle F_{n+1} fold.

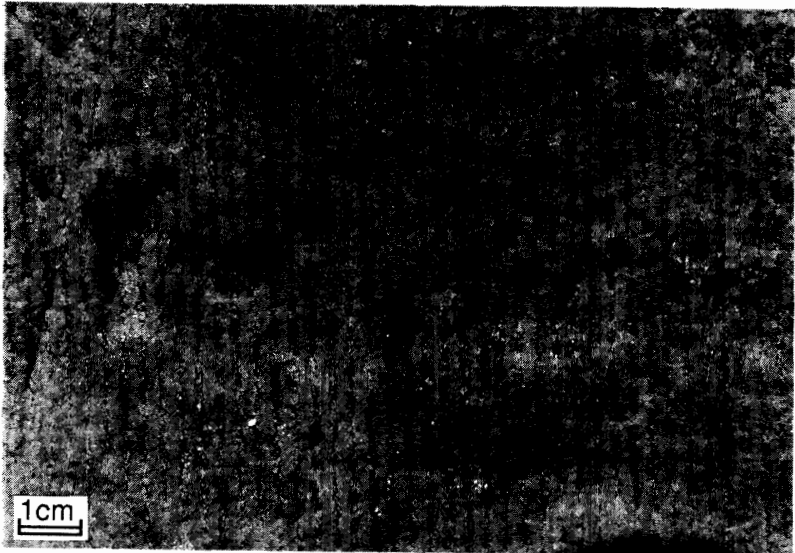


Fig. 19. Axial plane foliation of Bt in the hinge of F_{n+1} folds.



Fig. 20. Photomicrograph of axial plane foliation of Bt in the hinge of F_{n+1} fold. Plane polarized light. Sample no. J34-RN82-4.

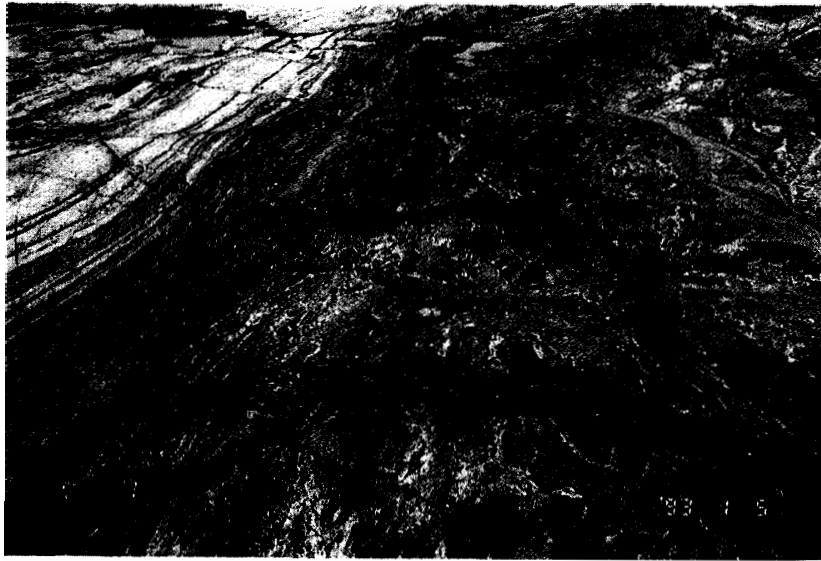


Fig. 21. Cpx pegmatites, intruded into parallel ruptures of Cpx-Opx-Hbl granulites, perpendicular to the dominant mineral lineation. The constituent minerals are Cpx, Hbl and a minor amount of Pl. Host rocks are boudinaged by parallel tension cracks.



Fig. 22. Clinopyroxene pegmatite, which did not intrude into Cpx-Opx-Hbl gneiss except near the lithological boundary. The host rocks are restricted to layers or alternation zones of pyroxene-rich granulites (e.g. Cpx-Opx-Hbl granulites). Thickness of Cpx pegmatite = 40 cm.



Fig. 23. Basic dykes. Gneisses and granulites were cut in places by basic dykes, of which the main constituent minerals are Cpx, Hbl and Pl (MOTOYOSHI et al., 1986). Thickness of basic dykes = 10 cm.



Fig. 24. Basic dykes cut F_n folds.



Fig. 25. Basic dykes, folded slightly with subvertical fold axial planes which are parallel to axial planes of F_{n+1} folds. This suggests that basic dyke intrusion took place in the late stage of F_{n+1} deformation phase.

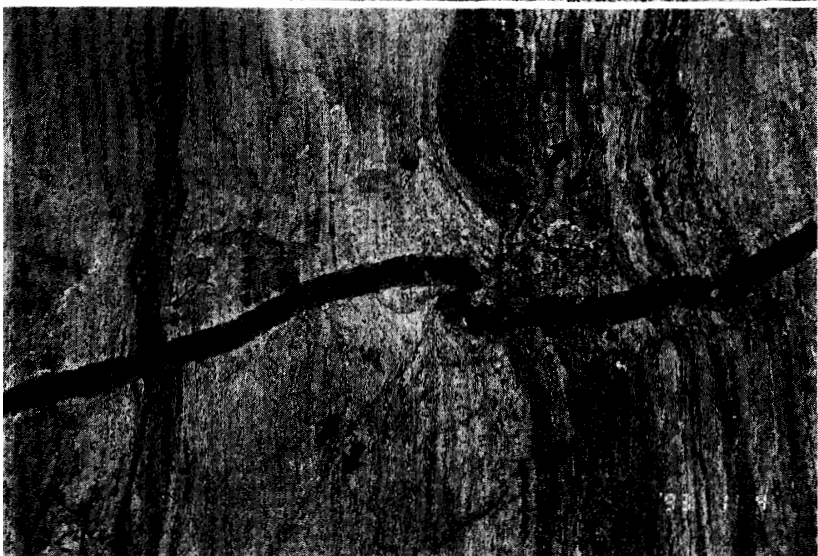


Fig. 26. Basic dyke, which was sheared locally by extensional narrow ductile shear zones. This indicates that basic dyke intrusion took place before extensional narrow shearing.



Fig. 27. Brittle boudinage and extensional narrow ductile shear zones. The narrow ductile shear zones are especially abundant in the Qtz-Pl-Kfs-rich gneiss (e.g. Grt-Sil gneiss, Grt-Bt gneiss and Cpx-Opx-Hbl-Bt gneiss). In contrast to these narrow ductile shear zones, strike-slip faults occurred in Cpx-Opx-Hbl granulites.

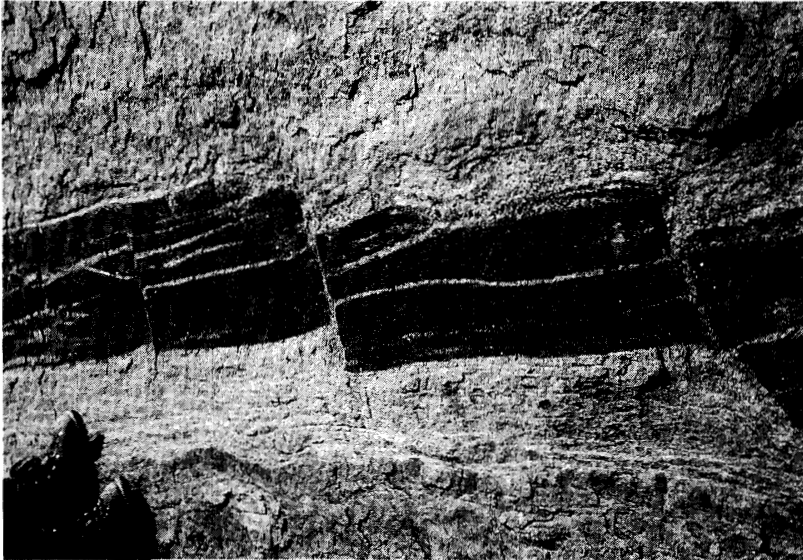


Fig. 28. Brittle boudinage. The narrow ductile shear zones were not developed.



Fig. 29. Narrow ductile shear zone in the Grt-Sil gneiss.



Fig. 30. Large-scale low-angle ductile thrust.

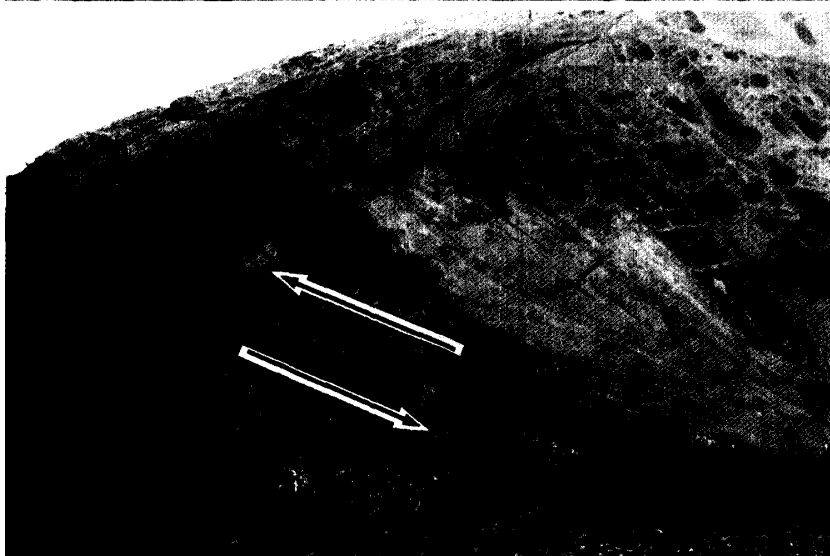


Fig. 31. Ductile thrust of outcrop-scale. Width of photo = 2 m.

Fig. 32. Felsic pegmatite, which cuts strike-slip ductile shear zone associated with thrusting. The orientation of the felsic pegmatite suddenly changes near the shear zone (left). However it was not affected by shearing because the pegmatite was not mylonitized at all. The felsic pegmatite was only intruded into a minor shear plane in the ductile shear zone.



stress field is estimated during emplacement of Cpx pegmatites and basic dykes. Therefore F_{n+1} folding, emplacement of Cpx pegmatites and basic dykes, and this extensional ductile shearing and faulting most likely took place in response to a single prolonged deformational episode represented by E-W extension and N-S compression.

5.2.4. Ductile thrusting

Geological mapping has demonstrated the presence of low angle ductile thrusts and related sub-vertical ductile shear zones in the northern part of Rundvågshetta (Figs. 1B, 30 and 31). The ductile thrusts cut mappable-scale F_{n+1} folds, indicating ductile thrusting took place after the time of F_{n+1} folding, emplacement of Cpx pegmatites and basic dykes. Along these ductile thrusts and associated strike-slip ductile shear zones, new penetrative foliations are developed (e.g. aligned Sil grains in Grt-Sil gneiss). Ductile thrust zones strike E-W and dip to the north at low angles, and drag patterns along ductile shear zones indicate that the northern upper part moved more than 50 m southward in the N-S compressional field. Moreover, small-scale strike-slip shear zones exhibit conjugacy, and suggest E-W extension and N-S compression.

Therefore F_{n+1} folds, extensional cracking associated with Cpx pegmatites and basic dykes, extensional-conjugate-narrow shear zones and ductile thrusts may have formed in response to a single prolonged deformational episode during cooling, because all indicate a N-S compressional field.

5.2.5. Emplacement of felsic pegmatite

The main constituent minerals of the felsic pegmatites are Qtz, Kfs, Pl with minor Bt, Hbl and Mt. The felsic pegmatites cross-cut F_n and F_{n+1} folds, Cpx pegmatites, basic dykes, extensional narrow shear zones and ductile thrusts in Rundvågshetta (Fig. 32). This shows that the emplacement of felsic pegmatites was the last event at Rundvågshetta. The felsic pegmatites are generally undeformed, but locally exhibit weak foliation defined by preferred orientation of Bt striking nearly E-W and dipping subvertically. This texture may suggest that felsic pegmatites were emplaced in the last stage of N-S compression.

6. Summary

The deformation history of metamorphic rocks at Rundvågshetta is schematically presented in Figs. 33 and 34, and it is summarized below.

Deformation during peak metamorphism : Opx + Sil \pm Qtz assemblages reveal high- T , high- P conditions for peak metamorphism of granulites of Rundvågshetta. WNW-ESE subhorizontal L_n fabrics and associated pervasive high-strain structures such as isoclinal buckling folds (F_n) and ductile boudinage (B_n and B_m) imply a regional ductile deformation during the high- T high- P (peak) metamorphism.

Crd after Opx + Sil \pm Qtz generally exhibits a weak preferred orientation subparallel to the dominant mineral lineation, but the form of the reaction texture itself is low-strained or undeformed. The Opx + Crd \pm Spr symplectic textures are also unstrained. The following low-strained and unstrained reaction textures suggest that the intense ductile deformation such as F_n folding and B_n ductile boudinage ceased before the time of the formation of reaction products (1) Crd reaction coronas after Opx + Sil + Qtz, (2) Crd + Spr symplectites after Opx + Sil, (3) Crd + Spr + Spl symplectites after Opx + Sil, (4) Opx + Crd symplectites after Grt + Qtz and (5) Opx + Crd + Spr symplectites after Grt.

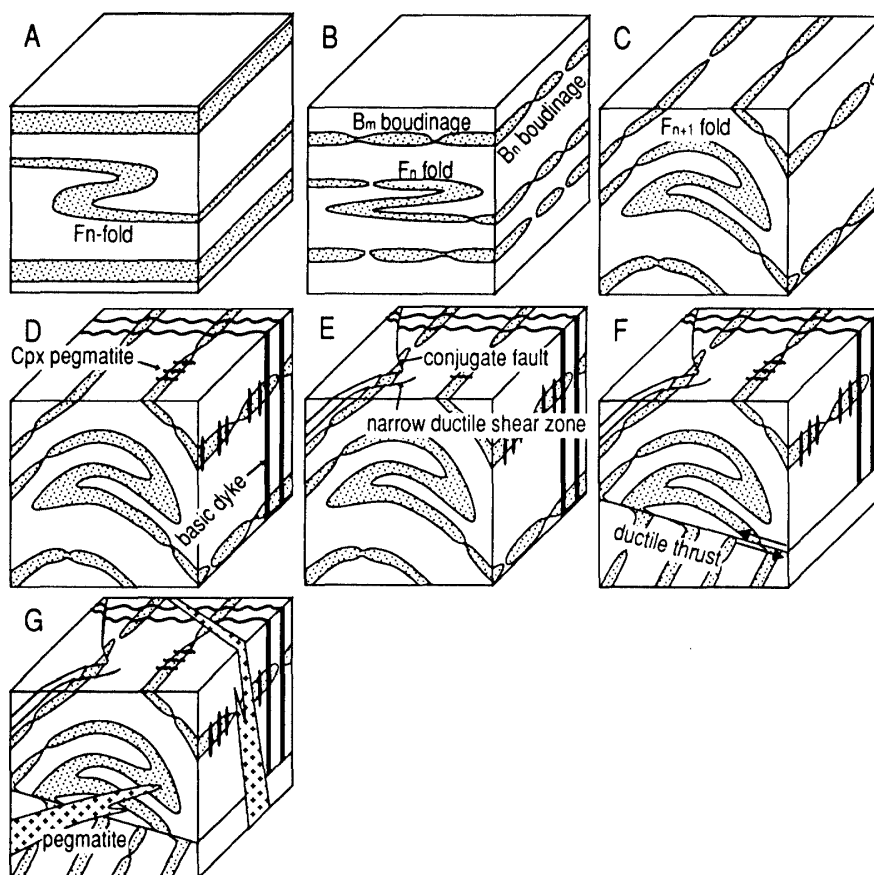


Fig. 33. Schematic illustration of structural evolution of Rundvågshetta. A : Deformation phase of isoclinal F_n folding. B : Strong ductile deformation (B_n , B_m and F_n) during $Opx + Sil \pm Qtz$ stable phase C : Deformation phase of F_{n+1} folding. D : Emplacement of Cpx pegmatite and basic dyke during later F_{n+1} fold event. E : Deformation phase of extensional narrow ductile shearing and faulting. F : Deformation phase of ductile thrusting. G : Emplacement phase of felsic pegmatite.

Deformation before peak metamorphism : Previous workers (ISHIKAWA, 1976 ; ISHIKAWA *et al.*, 1976, 1977 ; YOSHIDA, 1977, 1978; MATSUMOTO *et al.*, 1979, 1982) have recognized fold interference patterns which indicate multiple phases of ductile deformation throughout the Lützow-Holm Bay region. These generally include an isoclinal phase followed by a phase of upright, gentle folds. In this study, we recognize the existence of two earlier fold generations (F_{n-1} and F_{n-2}) which have not been described in those previous works. The F_{n-1} and F_{n-2} predating F_n are considered to be formed before peak metamorphism.

Deformation after peak metamorphism : The structural studies show that high-strain ductile deformation was followed by low-strain ductile deformation after peak metamorphism. Subsequent to peak metamorphism, reactions R1-R5 occurred. Low strain F_{n+1} folds formed during or after this period (Fig. 33C), providing weak preferred orientation of Crd within otherwise undeformed reaction textures. Post-peak metamorphic structures indicate a N-S compressional and E-W extensional deformation (Fig. 33D). During the

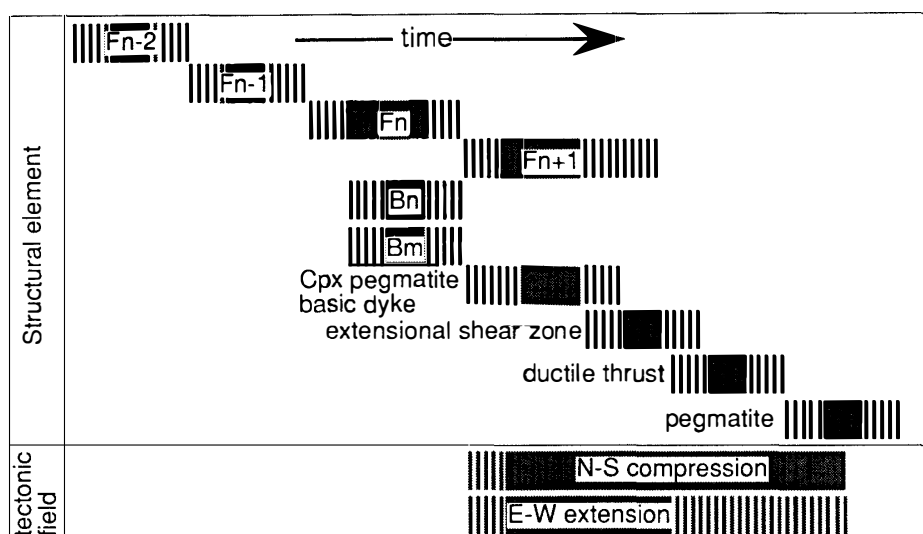


Fig. 34. Development of structural elements.

local development of ductile shear zones and faults, most quartzo-feldspathic lithologies behaved as ductile materials, but conjugate strike-slip or normal faulting took place in pyroxene-abundant granulites in preference to ductile shearing (Fig. 33E). The rheological behavior suggests cooling of metamorphic rocks. The extensional axis and compressional axis did not change during F_{n+1} folding, emplacement of Cpx pegmatites and basic dykes, and local extensional shearing. Due to subsequent N-S compression, ductile thrusts and strike-slip zones occurred at the northern part of the Rundvågshetta (Fig. 33F). After the ductile thrusting, felsic pegmatite were emplaced (Fig. 33G).

Acknowledgments

We wish to express our gratitude to all members of JARE-33 and -34 and the crew of icebreaker SHIRASE for their support during the 1991-1992 and 1992-1993 field seasons. Special thanks are due to Prof. K. SHIRAISHI (NIPR) and Dr. T. TOYOSHIMA (Niigata University) for reviews and a number of helpful suggestions.

References

- HIROI, Y., SHIRAISHI, K., YANAI, K. and KIZAKI, K. (1983): Aluminum silicates in the Prince Olav and Sôya Coasts, East Antarctica. *Mem. Natl Inst. Polar Res., Spec. Issue*, **28**, 115-131.
- HIROI, Y., SHIRAISHI, K., MOTOYOSHI, Y., KANISAWA, S., YANAI, K. and KIZAKI, K. (1986): Mode of occurrence, bulk chemical compositions, and mineral textures of ultramafic rocks in the Lützow-Holm Complex, East Antarctica. *Mem. Natl Inst. Polar Res., Spec. Issue*, **43**, 62-84.
- HIROI, Y., SHIRAISHI, K., MOTOYOSHI, Y. and KATSUSHIMA, T. (1987): Progressive metamorphism of calc-silicate rocks from the Prince Olav and Sôya Coasts, East Antarctica. *Proc. NIPR Symp. Antarct. Geosci.*, **1**, 73-97.
- HIROI, Y., SHIRAISHI, K. and MOTOYOSHI, Y. (1991): Late Proterozoic paired metamorphic complexes in East Antarctica, with special reference to the tectonic significance of ultramafic rocks. *Geological Evolution of Antarctica*, ed. by M.R.A. THOMSOM *et al.* Cambridge, Cambridge

- Univ. Press, 83–87.
- HOBBS, B.E., MEANS, W.D. and WILLIAMS, P.F. (1976): *An Outline of Structural Geology*. New York, J. Wiley, 571 p.
- ISHIKAWA, T. (1976): Superimposed folding of the Precambrian metamorphic rocks of the Lützow-Holm Bay region, East Antarctica. *Mem. Natl Inst. Polar Res., Ser. C (Earth Sci.)*, **9**, 41 p.
- ISHIKAWA, T., TATSUMI, T., KIZAKI, K., YANAI, K., YOSHIDA, M., ANDO, H., KIKUCHI, T., YOSHIDA, Y. and MATSUMOTO, Y. (1976): Geological map of Langhovde, Antarctica. *Antarct. Geol. Map Ser., Sheet 5 (with explanatory text 10 p.)*. Tokyo, Natl Inst. Polar Res.
- ISHIKAWA, T., YANAI, K., MATSUMOTO, Y., KIZAKI, K., KOJIMA, S., TATSUMI, T., KIKUCHI, T. and YOSHIDA, M. (1977): Geological map of Skarvsnes, Antarctica. *Antarct. Geol. Map Ser., Sheet 6 and 7 (with explanatory text 18 p.)*. Tokyo, Natl Inst. Polar Res.
- KAWASAKI, T., ISHIKAWA, M. and MOTOYOSHI, Y. (1993): Preliminary report on cordierite bearing assemblages from Rundvågshetta, Lützow-Holm Bay, East Antarctica: Evidence for a decompressional *P-T* path? *Proc. NIPR Symp. Antarct. Geosci.*, **6**, 47–56.
- KRETZ, R. (1983): Symbols for rock-forming minerals. *Am. Mineral.*, **68**, 277–279.
- MATSUMOTO, Y., YOSHIDA, M. and YANAI, K. (1979): Geology and geologic structure of the Langhovde and Skarvsnes regions, East Antarctica. *Mem. Natl Inst. Polar Res., Spec. Issue*, **14**, 106–120.
- MATSUMOTO, Y., NISHIDA, S., YANAI, K. and KOJIMA, H. (1982): Geology and geologic structure of the northern Ongul Islands and surroundings, East Antarctica. *Mem. Natl Inst. Polar Res., Spec. Issue*, **21**, 47–70.
- MOTOYOSHI, Y. (1986): Prograde and progressive metamorphism of the granulite-facies Lützow-Holm Bay region, East Antarctica. D. Sc. thesis, Hokkaido Univ., 238 p.
- MOTOYOSHI, Y., MATSUEDA, H., MATSUBARA, S., SASAKI, K. and MORIWAKI, K. (1986): Geological map of Rundvågskollane and Rundvågshetta, Antarctica. *Antarct. Geol. Map Ser., Sheet 24 (with explanatory text 11 p.)*. Tokyo, Natl Inst. Polar Res.
- MOTOYOSHI, Y., MATSUBARA, S. and MATSUEDA, H. (1989): *P-T* evolution of the granulite-facies rocks of the Lützow-Holm Bay region, East Antarctica. *Evolution of Metamorphic Belts*, ed. by J.S. DALY *et al.* Oxford, Blackwell, 325–329 (*Geol. Soc. Spec. Publ.*, No. 43).
- MOTOYOSHI, Y., ISHIKAWA, M., FRASER, G.L. and KAWASAKI, T. (1993): Metamorphism of the Lützow-Holm Complex revisited. *Dai-13-kai Nankyoku Chigaku Shinpojiumu Puroguramu. Kôen Yôshi (Prog. Abstr. 13th Symp. Antarct. Geosci.)*. Tokyo, Natl Inst. Polar Res., 62–63.
- NAKAJIMA, T., SHIBATA, K., SHIRAIISHI, K., MOTOYOSHI, Y. and HIROI, Y. (1988): Rb-Sr whole-rock ages of metamorphic rocks from Eastern Queen Maud Land, East Antarctica (2): Tenmondai Rock and Rundvågshetta (Abstract). *Proc. NIPR Symp. Antarct. Geosci.*, **2**, 172.
- SHIRAIISHI, K., HIROI, Y., MOTOYOSHI, Y. and YANAI, K. (1987): Plate tectonic development of late Proterozoic paired metamorphic complexes in eastern Queen Maud Land, East Antarctica. *Gondwana Six: Structure, Tectonics and Geophysics*, ed. by G.D. MCKENZIE. Washington, D.C., Am. Geophys. Union, 309–318 (*Geophys. Mon.* 40).
- SHIRAIISHI, K., ELLIS, D.J., HIROI, Y., FANNING, C.M., MOTOYOSHI, Y. and NAKAI, Y. (1994): Cambrian orogenic belt in East Antarctica and Sri Lanka: Implications for Gondwana assembly. *J. Geol.*, **102**, 47–65.
- YOSHIDA, M. (1977): Geology of the Skallen region, Lützow-Holmbukta, East Antarctica. *Mem. Natl Inst. Polar Res., Ser. C (Earth Sci.)*, **11**, 38 p.
- YOSHIDA, M. (1978): Tectonics and petrology of charnockites around Lützow-Holmbukta, East Antarctica. *J. Geosci., Osaka City Univ.*, **21**, 65–152.

(Received April 5, 1994; Revised manuscript received May 29, 1994)